

Molten lithium metal battery with $\text{Li}_4\text{Ti}_5\text{O}_{12}$ cathode and solid electrolyte

Yuanzheng Long^a, Jialiang Lang^{a,b}, Kai Liu^{c,**}, Kuangyu Wang^a, Yulong Wu^a, Haitian Zhang^b, Meicheng Li^c, Yang Jin^{d,***}, Xiangming He^b, Hui Wu^{a,*}

^a State Key Lab of New Ceramics and Fine Processing, School of Materials Science and Engineering, Tsinghua University, Beijing, 100084, PR China

^b Institute of Nuclear and New Energy Technology, Tsinghua University, Beijing, 100084, PR China

^c State Key Laboratory of Alternate Electrical Power System with Renewable Energy Sources, School of New Energy, North China Electric Power University, Beijing, 102206, PR China

^d Research Center of Grid Energy Storage and Battery Application, School of Electrical Engineering, Zhengzhou University, Zhengzhou, 450001, PR China

ARTICLE INFO

Keywords:

Energy storage system
Lithium metal battery
Lithium titanate
Solid electrolyte

ABSTRACT

Along with the rapid development of electric vehicles (EVs) and intermittent renewable energy, energy storage for EVs has received much attention over the past decade. Rechargeable batteries have been considered a feasible solution to utilize intermittent renewable energy with higher efficiency. Rechargeable batteries with promising safety, lifespan, low expenditure, durable components, or mature electric control systems are desired for energy storage systems. Recently, solid electrolyte-based liquid lithium (SELL) batteries have demonstrated excellent performances and great potential for energy storage applications by manipulating different cathode materials. Herein, a new type of SELL battery with $\text{Li}_4\text{Ti}_5\text{O}_{12}$ cathode (SELL-LTO battery) is reported. $\text{Li}_4\text{Ti}_5\text{O}_{12}$ is a distinctive electrode material with good rate performance, high-standard safety, moderate cost, and superior cycling stability at 280 °C, which make it an excellent cathode material for SELL batteries. The assembled SELL-LTO full cell has been cycled 100 times with an average energy efficiency of 92%. Moreover, the cell also exhibits good rate performance and can recover after being cooled and thawed.

1. Introduction

Lithium-ion batteries (LIBs) have been widely used in portable electronic devices, EVs, and energy storage systems [1–4]. Recently, the applications of LIBs in energy storage systems for EVs have intrigued considerable attention as intermittent new energy has been well developed, such as wind and solar energy [5–7]. However, some existing energy storage devices may not meet the strict requirements for EVs or large-scale smart grids, such as safety, long lifespan, robustness for discontinuous energy income, and high rate capability for developing energy storage systems for intermittent energy [7–9].

In the last two or three years, with the rapid growth of the electric vehicle and lithium battery markets, lithium resource prices have indeed fluctuated dramatically. This has resulted in high lithium prices today. However, scientists believe that the price of lithium resources could return to normal in the next 2–3 years [10]. Battery material recycling is expected to form a scale after 2030. Around 2050, the supply of raw

mineral resources and recycling resources will reach a comparable level, and in the longer term, recycling resources will wholly and gradually replace the demand for raw resources [11]. Furthermore, Lang et al. managed to achieve a low-cost recovery method for lithium metal resources, significantly reducing the extraction cost of lithium metal resources [12]. Considering the factors above, future energy storage systems for intermittent energy applying lithium resources still own promising prospects in saving carbon emissions and being economy-friendly.

In recent years, solid-state batteries applying garnet, polymer, sulfide, or other solid electrolytes are attracting more and more attention for their potential in energy storage [13–15]. Solid electrolyte-based liquid lithium (SELL) batteries, consisting of the molten lithium anode and solid electrolytes such as $\text{Li}_{6.4}\text{La}_3\text{Ta}_{0.6}\text{Zr}_{1.4}\text{O}_{12}$ (LLZTO), have already demonstrated a vast potential in serving as energy storage units [16–20]. In SELL batteries, molten liquid lithium is applied as anode materials, while LLZTO tubes serve as solid electrolyte. With the

* Corresponding author.

** Corresponding author.

*** Corresponding author.

E-mail addresses: liukai21@ncepu.edu.cn (K. Liu), yangjin@zzu.edu.cn (Y. Jin), huiwu@tsinghua.edu.cn (H. Wu).

liquid-solid interphase contact between molten lithium anode and LLZTO tubes, SELL batteries make the most of the high conductivity of solid electrolytes such as LLZTO [17,18,20]. SELL batteries using Sn-Pb, Bi-Pb, S, Se, and metal halides as cathodes have been reported by our team as well as other scientists in recent years [21–26]. By applying different cathode materials, these SELL batteries show advantages in rate capability, energy cost, and reliability. These various advantages could potentially assist the development of future EV energy storage.

Lithium titanate ($\text{Li}_4\text{Ti}_5\text{O}_{12}$), as a promising electrode material, has the potential to suffice stationary energy storage owing to its excellent cyclic stability, rate performance, and high-standard safety, especially for its stability in high temperatures where SELL batteries operate. Previous studies have shown proficient rate performance and electronic conductivity of $\text{Li}_4\text{Ti}_5\text{O}_{12}$ in traditional LIBs [27–30]. However, as a typical lithium-ion storage material, $\text{Li}_4\text{Ti}_5\text{O}_{12}$ is often applied as an anode material in conventional lithium-ion batteries due to its low charge-discharge plateau. Cathode materials in these batteries possess higher charge-discharge plateaus. As $\text{Li}_4\text{Ti}_5\text{O}_{12}$ still possesses a higher plateau than lithium metal anode, the SELL battery proves the capability for $\text{Li}_4\text{Ti}_5\text{O}_{12}$ to work as a cathode material.

Previous research often applies $\text{Li}_4\text{Ti}_5\text{O}_{12}$ at room temperature, but its electrochemistry performance at high temperatures has not been studied. Some research is devoted to exploring the performance of $\text{Li}_4\text{Ti}_5\text{O}_{12}$ batteries at various extreme temperatures, indicating that such materials are insensitive to temperature [5,31–34]. However, an electrochemistry device with a working temperature higher than 200 °C for $\text{Li}_4\text{Ti}_5\text{O}_{12}$ has not appeared. The chemical and electrochemical stability, good rate performance, and moderate cost indicate the possibility of applying $\text{Li}_4\text{Ti}_5\text{O}_{12}$ in our SELL batteries [35–38]. The electrochemical performance and stability of $\text{Li}_4\text{Ti}_5\text{O}_{12}$ at high temperatures also give scientists a deeper understanding of $\text{Li}_4\text{Ti}_5\text{O}_{12}$.

Herein, we designed a SELL-LTO ($\text{Li}|\text{LLZTO}|\text{Li}_4\text{Ti}_5\text{O}_{12}$) battery consisting of $\text{Li}_4\text{Ti}_5\text{O}_{12}$ as cathode, solid electrolyte (garnet-type $\text{Li}_{6.4}\text{La}_3\text{Ta}_{0.6}\text{Zr}_{1.4}\text{O}_{12}$ (LLZTO)), and liquid lithium as anode [39–44]. The SELL-LTO full cell achieved high cycling stability and rate performance with high energy and coulombic efficiency (>99.9%). Besides, the new-designed battery can be cooled down during operation and recovered after being thawed. Moreover, as a result of the inflammability of the electrolyte materials, there was no safety hazard even when the LLZTO tube was broken and a short circuit happened. By comparison, the theoretical energy cost of the SELL-LTO battery is lower than traditional LIBs. Therefore, we anticipate the SELL-LTO full cell extends the application of $\text{Li}_4\text{Ti}_5\text{O}_{12}$ -based batteries at a high temperature and has the potential for stationary energy storage.

2. Experimental

2.1. Fabrication of LLZTO ceramic tubes

Li_2CO_3 (Sinopharm Chemical Reagent Co., Ltd, 99.99%), La_2O_3 (Sinopharm Chemical Reagent Co., Ltd, 99.99%), ZrO_2 (Aladdin, 99.99%) and Ta_2O_5 (Ourchem, 99.99%) were mixed at the mole ratio of $\text{Li}_{6.5}\text{La}_3\text{Zr}_{0.5}\text{Ta}_{1.5}\text{O}_{12}$ (20% excess Li_2CO_3 were added) and then heated at 900 °C for 6 h. The as-prepared powders were milled for 12 h with a ball milling machine and then pressed into a U-shape tube under 220 MPa for 120 s with a cold isostatic press. The as-prepared tube was annealed at 1140 °C for 16 h in the air while being covered with the same mother powder.

2.2. Assemble and electrochemical measurement of SELL-LTO cell

$\text{Li}_4\text{Ti}_5\text{O}_{12}$ powder (0.18 g, Sinopharm Chemical Reagent Co., Ltd, 99.99%) and carbon black (0.02 g, Sinopharm Chemical Reagent Co., Ltd, 99.99%) were thoroughly mixed and dispersed in 5 mL ethyl alcohol. Then a carbon fiber felt was put into a stainless steel case. The as-prepared ethyl alcohol solution was dipped into the carbon fiber felt

and then dried for 10 h in an oven. After drying, the stainless steel case was transferred into an argon-filled glove box (Etelux, Lab2000). 1 g LiI-CsI salt (mole ratio 1:1) was added to the stainless steel case and heated for 1 h under 300 °C. Li foil (0.4 g, Alfa Aesar, 99.99%) was first put into an LLZTO tube and heated for 1 h under 300 °C in an argon-filled glove box to melt Li metal. Then a stainless steel stick was inserted into the melt Li as the negative current collector. The assembly process was conducted in an argon-filled glove box. The electrochemical tests of the SELL-LTO cells were conducted in an argon-filled box furnace (MTI) at 280 °C with the battery test system (LAND 2001 CT battery tester).

2.3. Characterization

The relative density of the LLZTO tube was measured by the Archimedes method. The microstructure of all the samples was investigated by scanning electron microscopy with a MERLIN Compact Zeiss scanning electron microscope. TEM observations were conducted on JEOL-ARM-200F TEM operated at 200 kV. The X-ray diffraction (XRD) patterns of the as-fabrication materials were evaluated using a D/max-2500 diffractometer (Rigaku, Japan) equipped with a CuK_α radiation source. Size distributions of $\text{Li}_4\text{Ti}_5\text{O}_{12}$ particles were studied using a Mastersize-2000 Malvern laser granularity analyzer. The impedance spectroscopy measurement was conducted with a broadband dielectric spectrometer (NOVOCOL) (frequency range: 10 MHz–40 Hz; AC voltage: 10 mV; temperature: 40–280 °C).

3. Results and discussion

3.1. Battery structure and material design

The SELL-LTO battery includes a $\text{Li}_4\text{Ti}_5\text{O}_{12}$ cathode, LLZTO solid electrolyte, and lithium anode. The configuration schematic of the battery is shown in Fig. 1a.

LLZTO ceramic tube functions as electrolyte and separator (Fig. 1b, c, d, Fig. S1). The contact between LLZTO and oxygen and carbon dioxide would lead to lithium carbonate production on the surface [45,46]. In order to avoid the side effects of these by-products for the battery, LLZTO is used after careful polishing. Because of the high relative density of the LLZTO ceramic tube (99%) [41,42,47], leakage or crossover of the liquid electrode materials and the self-discharge of the battery can be effectively restrained.

The carbon fiber felt is used as the cathode current collector, and the carbon black powder is used as the conductive additive. The molten salt (LiI-CsI) is used as the secondary electrolyte for Li-ion transporting to enhance the contact between the cathode and LLZTO solid electrolyte [48–50].

Carbon-coated $\text{Li}_4\text{Ti}_5\text{O}_{12}$ particles are used as cathode materials (Fig. 2) to improve the electronic conductivity of the cathode. The SEM images of $\text{Li}_4\text{Ti}_5\text{O}_{12}$ particles demonstrate their microscopic appearance (Fig. 2a and b). As shown in Fig. 2c, the thickness of the carbon layer is about 5 nm. Fig. 2d, e, f, and Fig. S2 demonstrate that the $\text{Li}_4\text{Ti}_5\text{O}_{12}$ particles in the SELL-LTO battery own a standard phase and promising electrochemistry cycling performance.

Because of the high operating temperature, the lithium anode retains its liquid state and therefore keeps a good soakage ability with the solid electrolyte. Besides, the solid electrolyte exhibits a high ionic conductivity of 95 mS cm^{-1} at the running temperature (280 °C, Fig. 1d), which is nearly ten times higher than that of most liquid organic electrolytes at room temperature (e.g., ~10 mS cm^{-1} , 1 M LiPF₆ in carbonate-based solvent).

Attributed to our non-flammable cathode materials, our battery system demonstrates high safety. Even when a crack appeared in the ceramic tube, rapid chemical reactions would not happen when cathode and anode materials were mixed together. When the LLZTO tube was broken deliberately during operation and the liquid Li metal directly reacted with the cathode, the surface temperature of the cell only

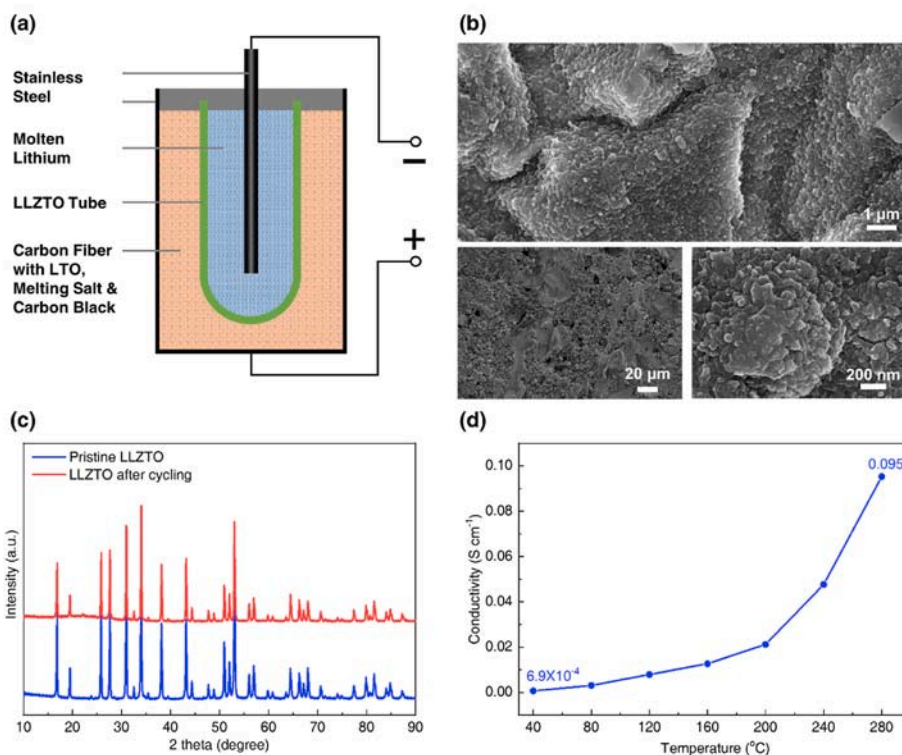


Fig. 1. (a) Schematic of the SELL-LTO cell; (b) SEM image of the pristine LLZTO ceramic; (c) XRD patterns of the LLZTO before and after cycling; (d) the ionic conductivity of LLZTO ceramic from 40 to 280 °C.

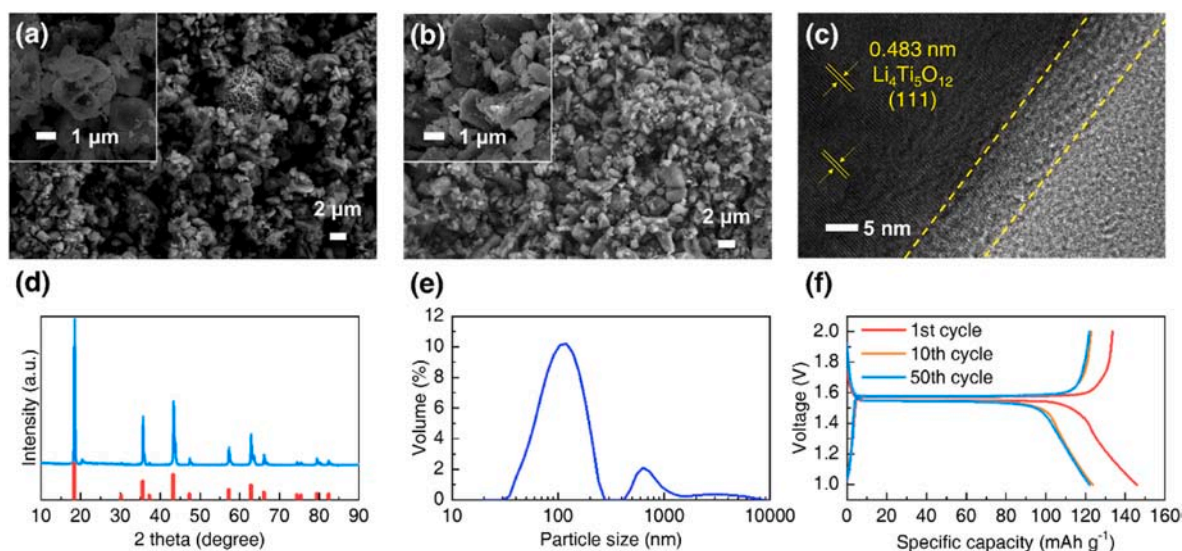


Fig. 2. (a) SEM image of the pristine $\text{Li}_4\text{Ti}_5\text{O}_{12}$ particles before cycling; (b) SEM image of the pristine $\text{Li}_4\text{Ti}_5\text{O}_{12}$ particles after cycling; (c) TEM images of the pristine $\text{Li}_4\text{Ti}_5\text{O}_{12}$ particles. Yellow dashed lines mark the carbon layer; (d) XRD pattern of the pristine $\text{Li}_4\text{Ti}_5\text{O}_{12}$ particles; (e) Size distribution of the pristine $\text{Li}_4\text{Ti}_5\text{O}_{12}$ particles; (f) The cycling performance of the LTO || Li cell with organic electrolyte in room temperature. Voltage profiles of the 1st, 10th, and 50th discharge/charge cycles at 1 mA cm^{-2} . (For interpretation of the references to colour in this figure legend, the reader is referred to the Web version of this article.)

increased by a few dozen degrees, indicating the high safety of the batteries (Fig. S3).

3.2. SELL-LTO cell cycling performance

A SELL-LTO full cell was cycled at a current density of 5 mA cm^{-2} (equal to a rate of 0.25C) for 100 cycles (over a month) to test the cyclic performance. As shown in Fig. 3a, the specific capacity of $\text{Li}_4\text{Ti}_5\text{O}_{12}$ stabilized around 130 mAh g^{-1} after the 10th cycle. The charge and

discharge energy profile and the energy efficiency of the first 100 cycles are presented in Fig. 3b, indicating an average energy efficiency of 92% (Fig. S4).

The voltage profiles of the 10th, 50th, and 100th are shown in Fig. 3c. There is a broad discharge plateau from 1.6 V to 1.2 V, which is different from the discharge plateau of $\text{Li}_4\text{Ti}_5\text{O}_{12}$ batteries at room temperature (a flat plateau at $\sim 1.5 \text{ V}$) (Fig. 2f). Previous studies indicate two successive order-disorder phase transitions in $\text{Li}_4\text{Ti}_5\text{O}_{12}$ at a temperature above $177 \text{ }^\circ\text{C}$, which, we suspect, may lead to the change of

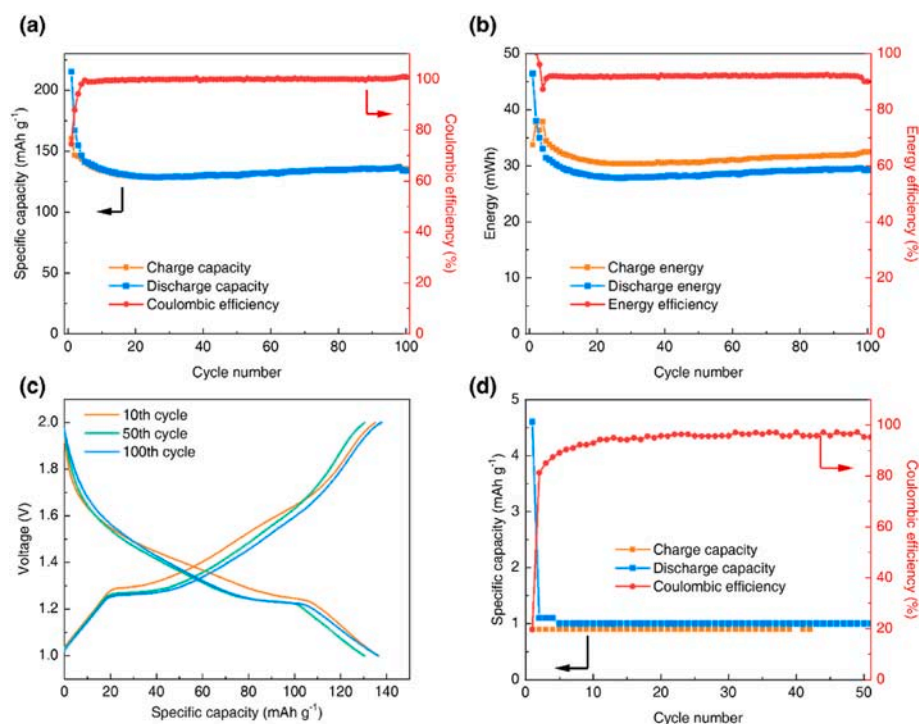


Fig. 3. Cycling performance of the SELL-LTO cell. (a) Specific capacity of the cathode and coulombic efficiency as functions of cycle number from the 1st cycle to the 100th cycle at 5 mA cm^{-2} ; (b) Charge and discharge energy, energy density as functions of cycle number from the 1st cycle to the 100th cycle at 5 mA cm^{-2} ; (c) Voltage profiles of the 10th, 50th, and 100th discharge/charge cycles at 5 mA cm^{-2} . (d) Specific capacity of carbon fiber felt and coulombic efficiency as functions of cycle number from the 1st cycle to the 50th cycle at 5 mA cm^{-2} . The upper limit of charge voltage is 2 V and the lower limit of discharge voltage is 1 V.

the discharge profiles of the SELL-LTO battery [27].

After the first 10 cycles, the battery's capacity stabilized and showed no obvious decay for the subsequent 80 cycles. The average coulombic efficiency of the full cell from the 5th cycle to the 100th cycle is higher than 99.9%, which demonstrates the promising quality of the solid electrolyte tube and good cycle stability of the full battery.

Moreover, the average energy efficiency of the full battery is 92%, which is as high as that of Li-ion batteries operating at room temperature [27]. The energy efficiency of the batteries is related to the cost of energy storage, and the high energy efficiency could effectively lower the cost.

3.3. Discussion about battery components

The stability of the LLZTO ceramic tube is also a critical factor affecting the lifespan of the full cell. XRD test was conducted on the LLZTO solid electrolyte at the pristine state and after 100 cycles. As shown in Fig. 1c, there is no apparent change in the XRD patterns of LLZTO before and after cycling, indicating the phase stability of LLZTO during cycling.

To verify that the carbon fiber felt and the molten LiI-CsI only function as the current collector and second electrolyte that provide no capacity, the cell without $\text{Li}_4\text{Ti}_5\text{O}_{12}$ powder was assembled and tested. As shown in Fig. 3d, the cell delivered a shallow capacity. Based on the result, the carbon fiber felt and the molten LiI-CsI contributed less than 1% of the capacity of the SELL-LTO full battery. Therefore, almost all the cathode capacity is contributed by the $\text{Li}_4\text{Ti}_5\text{O}_{12}$.

3.4. Features of SELL-LTO batteries

High-rate capability is necessary for batteries applied in energy storage units. The rate performance of the SELL-LTO cell is shown in Fig. 4. The battery was tested at various rates from 0.25C to 2.5C (i.e. at current densities from 5 mA cm^{-2} to 50 mA cm^{-2}). Even at a high current density of 50 mA cm^{-2} , the battery delivered an excellent cycling performance with a specific capacity of 90 mAh g^{-1} . After cycling at 50 mA cm^{-2} , the capacity of $\text{Li}_4\text{Ti}_5\text{O}_{12}$ rebounded to 130 mAh

g^{-1} and kept stable when the current density was reduced to 5 mA cm^{-2} , which indicates the excellent rate performance of the SELL-LTO battery. The excellent rate performance partly benefits from the high operating temperature. Not only the ionic conductivity of the LLZTO tube, but the ionic and electronic conductivity of $\text{Li}_4\text{Ti}_5\text{O}_{12}$ also improved significantly at the high temperature of $280 \text{ }^\circ\text{C}$ compared with those at room temperature [2,51–53] (Fig. S5). Therefore, the SELL-LTO battery exhibits a promising rate capability for potential application to energy storage systems in EVs.

The ability of the high-temperature battery to recover after being cooled down is also essential for their practical applications in the energy storage system [8,54,55]. The volume change during the freeze-reheat process of electrodes may cause mechanical failure of solid electrolytes, possibly leading to short circuits and even severe safety hazards of high-temperature batteries [56]. To investigate the stability of the SELL-LTO battery after freezing and thawing, cooling and thawing test of the battery was conducted, and the result is shown in Fig. 4c.

After the charging process, the battery was cooled down to room temperature and then reheated to $280 \text{ }^\circ\text{C}$ after about 15 h. After the temperature was preserved at $280 \text{ }^\circ\text{C}$, the battery was restarted and began to discharge. There was no short circuit or fluctuation in the subsequent discharge voltage curve. The following cycles kept stable, indicating that no failure of the full cell happened and the cell operated well after cooling and reheating.

Compared to some former SELL batteries and other high-temperature energy storage systems, SELL-LTO is safer and owns a discharge voltage of around 1.4V. $\text{Li}_4\text{Ti}_5\text{O}_{12}$ shows its advantages of more reasonable cost and higher energy efficiency. As SELL is an energy storage system family that can widely use different substances as cathode materials and can be enriched continuously, SELL-LTO also expands the family of SELL members.

Therefore, our SELL-LTO batteries overcome the two main problems of garnet solid electrolytes: low ionic conductivity when working at room temperature and high interface impedance caused by solid-solid contact. Moreover, most of the drawbacks of room-temperature Li metal batteries, such as Li dendrite growth and side reactions between Li metal and organic liquid electrolytes, do not exist in our cells. Hence, the

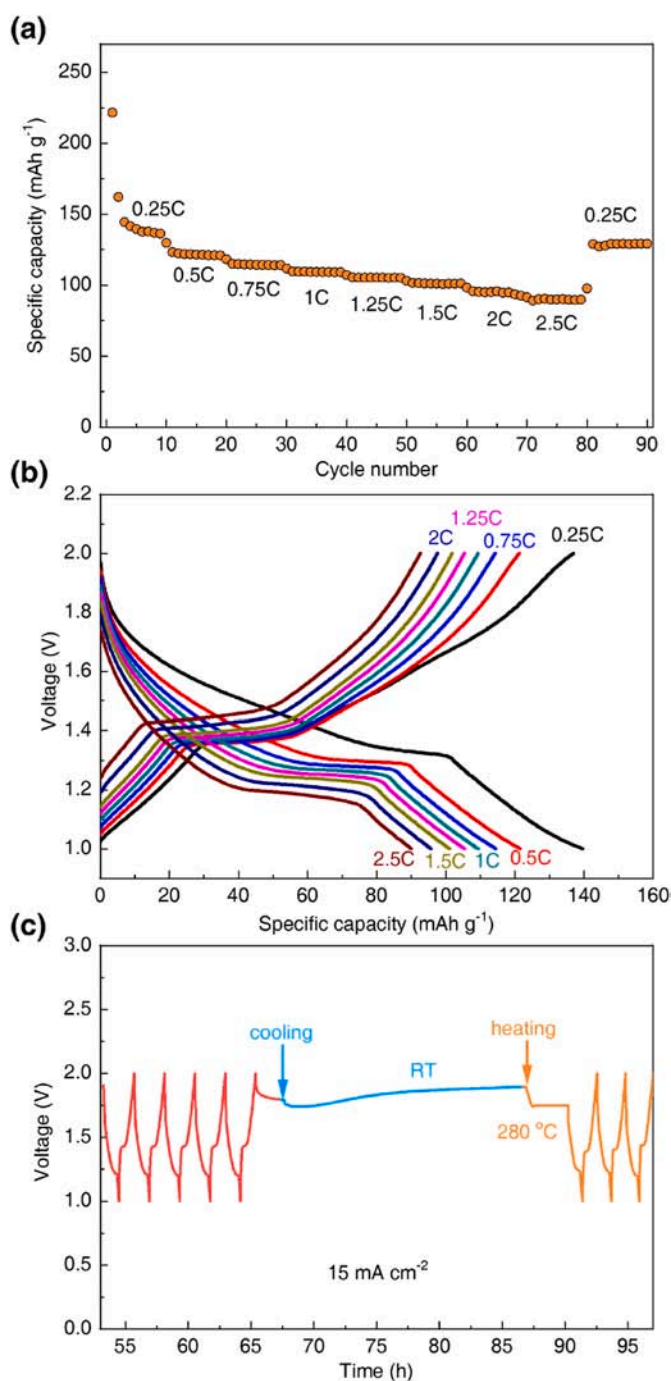


Fig. 4. Rate performance and heat recovery test of the SELL-LTO cell. (a) Specific capacity of the cathode as a function of cycle number at various C rates (2.5C equals to a current density of 50 mA cm⁻²); (b) Voltage profiles of the discharge/charge cycles at various C rates. (c) Freezing and thawing test of a SELL-LTO cell.

cyclic stability of the Li anode in the SELL-LTO full cell is quite promising.

3.5. Discussion on the application prospects of SELL-LTO

Although the SELL-LTO batteries operate at high temperatures (280 °C), requiring some equipment insulation, it is not a waste of energy when considering SELL-LTO for future large-scale energy storage.

Heat loss can be reduced by incorporating already available insulation with promising insulation and very low thermal conductivity. A

silica nanofiber mat that can be prepared in macro quantities and has an extremely low thermal conductivity (0.026 W m⁻¹ K⁻¹) has been developed [57]. This material has been shown to prevent the diffusion of heat significantly. When our SELL-LTO cells are used in combination with this material, on the one hand, heat loss after the cell is heated up is minimized. On the other hand, we can avoid the rapid heat transfer from a single cell to the other cells in the event of thermal runaway to cause catastrophic consequences. Furthermore, when SELL-LTO cells are used on a large scale, the thermal management of the battery pack can reduce the heat loss even less.

Future SELL-LTO large-scale energy storage fields should be built in neighborhoods with low electricity costs and abundant industrial waste heat. SELL-LTO focuses on the future needs of smart grid construction. Regions with low electricity costs often possess industries that emit a huge amount of waste heat. The waste heat will not only cause waste of resources but also cause the area's temperature to rise and thus affect the local ecological environment. In China, low-temperature waste heat below 300 °C accounts for more than 66% of the total waste heat [58]. The waste heat is suitable for the operation of SELL-LTO cells.

The construction of SELL-LTO cells is also cost-effective and economy friendly. Table 1 compares the production cost of different battery systems based on the latest market offer. Compared with LiCoO₂/C₆ battery and LiFePO₄/C₆ battery, the SELL-LTO battery is lower in cost than LiCoO₂/C₆ battery, although slightly higher than LiFePO₄/C₆ battery. Though lithium metal may be more expensive recently, in the long run, the price of lithium metal will return to a rational and reasonable range, which will be conducive to the promotion and large-scale use of SELL system batteries. Compared to previous SELL batteries, SELL-LTO also demonstrates no obvious shortage. Furthermore, the lithium metal recycling technology we developed can also form a closed loop with all kinds of batteries of the SELL system to reduce the overall cost.

In summary, even though our prototype battery currently requires a laboratory muffle furnace, the insulation and safety of the battery can be guaranteed in the future scenario of using it for large-scale energy storage and smart grid. Its construction location will be in areas with low electricity costs, industrial waste heat, and insulation materials. Moreover, the ingenuity of this design is that the exact match of its features and its application scenario happens to be endogenous and natural. Therefore, the insulation and heat consumption of SELL-LTO is an issue that needs attention but will not affect its use in future application scenarios.

4. Conclusions

In summary, we designed a novel SELL-LTO battery with Li₄Ti₅O₁₂ cathode, LLZTO solid electrolyte, and a molten lithium anode with high safety, higher energy efficiency, and remarkable rate capability. The full cell delivered an average energy efficiency of 92% at a current density of 5 mA cm⁻². Li₄Ti₅O₁₂ was first applied as a cathode material and at a high temperature. The SELL-LTO expands the family members of SELL. We propose that the cathode materials could expand to other electrode materials with higher operating voltage and energy density, such as LiCoO₂ or LiFePO₄. We anticipate our SELL-LTO battery will provide new choices for energy storage systems and high-temperature power sources.

CRediT authorship contribution statement

Yuanzheng Long: Conceptualization, Formal analysis, Investigation, Writing – original draft, Writing – review & editing. **Jiali Lang:** Conceptualization, Formal analysis, Investigation, Writing – original draft, Writing – review & editing. **Kai Liu:** Conceptualization, Formal analysis, Writing – original draft, Writing – review & editing. **Kuangyu Wang:** Investigation, Writing – original draft. **Yulong Wu:** Investigation, Writing – original draft. **Haitian Zhang:** Investigation, Writing – original draft. **Meicheng Li:** Investigation, Writing – original draft.

Table 1

Comparison of the production cost of different battery systems.

Battery system	Cathode	Cost (\$)	Anode	Cost (\$)	Capacity (Ah)	Average Voltage (V)	Total cost (\$)	Cost per kWh (\$)
SELL-LTO	5514 g Li ₄ Ti ₅ O ₁₂	78	250 g Li	21	965	1.5	99	68
LCO-C	7056 g LiCoO ₂	597	2592 g C ₆	22	965	3.7	619	173
LFPO-C	7110 g LiFePO ₄	170	2592 g C ₆	22	965	3.2	192	62
SELL-Se [21]	1422 g Se	104	250 g Li	21	965	2.0	125	65
SELL-SnPb [22]	2817 g Sn ₁₅ Pb ₅	37	250 g Li	21	965	0.47	58	128
SELL-BiPb [22]	2728 g Bi ₃ Pb	23	250 g Li	21	965	0.7	44	65
SELL-AlCl ₃ /LiCl [23]	324 g Al + 2035 g LiCl	183	250 g Li	21	965	1.55	204	136
SELL-brass/ZnCl ₂ [24]	1526 g LiCl + 1177 g Zn	142	250 g Li	21	965	2.1	163	80

Yang Jin: Writing – original draft, Writing – review & editing.
Xiangming He: Writing – review & editing. **Hui Wu:** Conceptualization, Formal analysis, Writing – original draft, Writing – review & editing, Supervision, Project administration.

Declaration of competing interest

The authors declare that they have no known competing financial interests or personal relationships that could have appeared to influence the work reported in this paper.

Data availability

Data will be made available on request.

Acknowledgments

This work was supported by the Basic Science Center Program of the National Natural Science Foundation of China (NSFC) under Grant No. 51788104, and Beijing Natural Science Foundation under Grant No. JQ19005. Y. L. would like to thank the grant support from Tsinghua University Initiative Scientific Research Program. Y.L. would specially thank his newlywed wife. The author team would thank Mr. Zhou, the engineer and the secretary of the team. Y. L. and J. L. contributed equally to this work.

Appendix A. Supplementary data

Supplementary data to this article can be found online at <https://doi.org/10.1016/j.etrans.2023.100235>.

References

- Goodenough JB, Kim Y. Challenges for rechargeable Li batteries. *Chem Mater* 2010;22(3):587–603. <https://doi.org/10.1021/cm901452z>.
- Tarascon JM, Armand M. Issues and challenges facing rechargeable lithium batteries. *Nature* 2001;414(6861):359–67. <https://doi.org/10.1038/35104644>.
- Li Y, Lu Y, Zhao C, Hu Y-S, Titirici M-M, Li H, Huang X, Chen L. Recent advances of electrode materials for low-cost sodium-ion batteries towards practical application for grid energy storage. *Energy Storage Mater* 2017;7:130–51. <https://doi.org/10.1016/j.ensm.2017.01.002>.
- Yu W, Guo Y, Shang Z, Zhang Y, Xu S. A review on comprehensive recycling of spent power lithium-ion battery in China. *eTransportation* 2022;11. <https://doi.org/10.1016/j.etrans.2022.100155>.
- Qian K, Tang L, Wagemaker M, He Y-B, Liu D, Li H, Shi R, Li B, Kang F. A facile surface reconstruction mechanism toward better electrochemical performance of Li₄Ti₅O₁₂ in lithium-ion battery. *Adv Sci* 2017;4(11). <https://doi.org/10.1002/advs.201700205>.
- Wang Y, Cao G. Developments in nanostructured cathode materials for high-performance lithium-ion batteries. *Adv Mater* 2008;20(12):2251–69. <https://doi.org/10.1002/adma.200702242>.
- Zhou L, Zhang K, Hu Z, Tao Z, Mai L, Kang Y-M, Chou S-L, Chen J. Recent developments on and prospects for electrode materials with hierarchical structures for lithium-ion batteries. *Adv Energy Mater* 2018;8(6). <https://doi.org/10.1002/aenm.201701415>.
- Dai T, Yang L, Ning XH, Zhang DL, Narayan RL, Li J, Shan ZW. A low-cost intermediate temperature Fe/Graphite battery for grid-scale energy storage. *Energy Storage Mater* 2020;25:801–10. <https://doi.org/10.1016/j.ensm.2019.09.008>.
- Wang Y, Wang L, Li M, Chen Z. A review of key issues for control and management in battery and ultra-capacitor hybrid energy storage systems. *eTransportation* 2020;4. <https://doi.org/10.1016/j.etrans.2020.100064>.
- Tian YS, Zeng GB, Rutt A, Shi T, Kim H, Wang JY, Koettgen J, Sun YZ, Ouyang B, Chen TN, Lun ZY, Rong ZQ, Persson K, Ceder G. Promises and challenges of next-generation "beyond Li-ion" batteries for electric vehicles and grid decarbonization. *Chem Rev* 2021;121(3):1623–69. <https://doi.org/10.1021/acs.chemrev.0c00767>.
- Makuz B, Tian Q, Guo X, Chattopadhyay K, Yu D. Pyrometallurgical options for recycling spent lithium-ion batteries: a comprehensive review. *J Power Sources* 2021;491. <https://doi.org/10.1016/j.jpowsour.2021.229622>.
- Lang JL, Jin Y, Liu K, Long YZ, Zhang HT, Qi LH, Wu H, Cui Y. High-purity electrolytic lithium obtained from low-purity sources using solid electrolyte. *Nat Sustain* 2020;3(5):386–90. <https://doi.org/10.1038/s41893-020-0485-x>.
- Wang ZY, Shen L, Deng SG, Cui P, Yao XY. 10 μm m-thick high-strength solid polymer electrolytes with excellent interface compatibility for flexible all-solid-state lithium-metal batteries. *Adv Mater* 2021;33(25). <https://doi.org/10.1002/adma.202100353>.
- Wen JY, Huang LQ, Huang Y, Luo W, Huo HY, Wang ZF, Zheng XY, Wen ZY, Huang YH. A lithium-MXene composite anode with high specific capacity and low interfacial resistance for solid-state batteries. *Energy Storage Mater* 2022;45:934–40. <https://doi.org/10.1016/j.ensm.2021.12.033>.
- Wu JH, Liu SF, Han FD, Yao XY, Wang CS. Lithium/sulfide all-solid-state batteries using sulfide electrolytes. *Adv Mater* 2021;33(6). <https://doi.org/10.1002/adma.202000751>.
- Huo HY, Chen Y, Li RY, Zhao N, Luo J, da Silva JGP, Mucke R, Kaghazchi P, Guo XX, Sun XL. Design of a mixed conductive garnet/Li interface for dendrite-free solid lithium metal batteries. *Energy Environ Sci* 2020;13(1):127–34. <https://doi.org/10.1039/c9ee01903k>.
- Samson AJ, Hofstetter K, Bag S, Thangadurai V. A bird's-eye view of Li-stuffed garnet-type Li₇La₃Zr₂O₁₂ ceramic electrolytes for advanced all-solid-state Li batteries. *Energy Environ Sci* 2019;12(10):2957–75. <https://doi.org/10.1039/c9ee01548e>.
- Guo QY, Xu FL, Shen L, Wang ZY, Wang J, He H, Yao XY. Poly(ethylene glycol) brush on Li_{6.4}La₃Zr_{1.4}Ta_{0.6}O₁₂ towards intimate interfacial compatibility in composite polymer electrolyte for flexible all-solid-state lithium metal batteries. *J Power Sources* 2021;498. <https://doi.org/10.1016/j.jpowsour.2021.229934>.
- Jia MY, Zhao N, Huo HY, Guo XX. Comprehensive investigation into garnet electrolytes toward application-oriented solid lithium batteries. *Electrochemical Energy Reviews* 2020;3(4):656–89. <https://doi.org/10.1007/s41918-020-00076-1>.
- Guo Q, Xu F, Shen L, Deng S, Wang Z, Li M, Yao X. 20 μm-thick Li_{6.4}La₃Zr_{1.4}Ta_{0.6}O₁₂-based flexible solid electrolytes for all-solid-state lithium batteries. *Energy Material Advances* 2022;9753506. <https://doi.org/10.34133/2022/9753506>. 2022.
- Jin Y, Liu K, Lang JL, Jiang X, Zheng ZK, Su QH, Huang ZY, Long YZ, Wang CA, Wu H, Cui Y. High-energy-density solid-electrolyte-based liquid Li-S and Li-Se batteries. *Joule* 2020;4(1):262–74. <https://doi.org/10.1016/j.joule.2019.09.003>.
- Jin Y, Liu K, Lang JL, Zhuo D, Huang ZY, Wang CA, Wu H, Cui Y. An intermediate temperature garnet-type solid electrolyte-based molten lithium battery for grid energy storage. *Nat Energy* 2018;3(9):732–8. <https://doi.org/10.1038/s41560-018-0198-9>.
- Lang JL, Liu K, Jin Y, Long YZ, Qi LH, Wu H, Cui Y. A molten battery consisting of Li metal anode, AlCl₃-LiCl cathode and solid electrolyte. *Energy Storage Mater* 2020;24:412–6. <https://doi.org/10.1016/j.ensm.2019.07.027>.
- Liu K, Lang JL, Yang MZ, Xu J, Sun B, Wu YL, Wang KY, Zheng ZK, Huang ZY, Wang CA, Wu H, Jin Y, Cui Y. Molten lithium-brass/zinc chloride system as high-performance and low-cost battery. *Matter* 2020;3(5):1714–24. <https://doi.org/10.1016/j.matt.2020.08.022>.
- Wang CW, Fu K, Kammampata SP, McOwen DW, Samson AJ, Zhang L, Hitz GT, Nolan AM, Wachsmann ED, Mo YF, Thangadurai V, Hu LB. Garnet-type solid-state electrolytes: materials, interfaces, and batteries. *Chem Rev* 2020;120(10):4257–300. <https://doi.org/10.1021/acs.chemrev.9b00427>.
- Zhang Q, Cai LT, Liu GZ, Li QH, Jiang M, Yao XY. Selenium-infused ordered mesoporous carbon for room-temperature all-solid-state lithium-selenium batteries with ultrastable cyclability. *ACS Appl Mater Interfaces* 2020;12(14):16541–7. <https://doi.org/10.1021/acsami.0c01996>.
- Zhao B, Ran R, Liu M, Shao Z. A comprehensive review of Li 4 Ti 5 O 12 -based electrodes for lithium-ion batteries: the latest advancements and future perspectives. *Mater Sci Eng R Rep* 2015;98:1–71. <https://doi.org/10.1016/j.mser.2015.10.001>.

- [28] Vijayakumar M, Kerisit S, Rosso KM, Burton SD, Sears JA, Yang Z, Graff GL, Liu J, Hu J. Lithium diffusion in Li₄Ti₅O₁₂ at high temperatures. *J Power Sources* 2011; 196(4):2211–20. <https://doi.org/10.1016/j.jpowsour.2010.09.060>.
- [29] Fehr KT, Holzapfel M, Laumann A, Schmidbauer E. DC and AC conductivity of Li₄/3Ti₅/304 spinel. *Solid State Ionics* 2010;181(23–24):1111–8. <https://doi.org/10.1016/j.ssi.2010.05.026>.
- [30] Zhang W, Topsakal M, Cama C, Pelliccione CJ, Zhao H, Ehrlich S, Wu LJ, Zhu YM, Frenkel AI, Takeuchi KJ, Takeuchi ES, Marschilok AC, Lu DY, Wang F. Multi-stage structural transformations in zero-strain lithium titanate unveiled by in situ X-ray absorption fingerprints. *J Am Chem Soc* 2017;139(46):16591–603. <https://doi.org/10.1021/jacs.7b07628>.
- [31] Rodrigues M-TF, Kalaga K, Gullapalli H, Babu G, Reddy ALM, Ajayan PM. Hexagonal boron nitride-based electrolyte composite for Li-ion battery operation from room temperature to 150 °C. *Adv Energy Mater* 2016;6(12). <https://doi.org/10.1002/aenm.201600218>.
- [32] Rodrigues M-TF, Babu G, Gullapalli H, Kalaga K, Sayed FN, Kato K, Joyner J, Ajayan PM. A materials perspective on Li-ion batteries at extreme temperatures. *Nat Energy* 2017;2(8). <https://doi.org/10.1038/nenergy.2017.108>.
- [33] Reddy MV, Subba Rao GV, Chowdari BV. Metal oxides and oxyalts as anode materials for Li ion batteries. *Chem Rev* 2013;113(7):5364–457. <https://doi.org/10.1021/cr3001884>.
- [34] Lin X, Salari M, Arava LM, Ajayan PM, Grinstaff MW. High temperature electrical energy storage: advances, challenges, and frontiers. *Chem Soc Rev* 2016;45(21): 5848–87. <https://doi.org/10.1039/c6cs00012f>.
- [35] Liu Y, Lin D, Yuen PY, Liu K, Xie J, Dauskardt RH, Cui Y. An artificial solid electrolyte interphase with high Li-ion conductivity, mechanical strength, and flexibility for stable lithium metal anodes. *Adv Mater* 2017;29(10). <https://doi.org/10.1002/adma.201605531>.
- [36] Xu P, Hu X, Liu X, Lin X, Fan X, Cui X, Sun C, Wu Q, Lin X, Yuan R, Zheng M, Dong Q. A lithium-metal anode with ultra-high areal capacity (50 mAh cm⁻²) by gridding lithium plating/stripping. *Energy Storage Mater* 2021;38:190–9. <https://doi.org/10.1016/j.ensm.2021.03.010>.
- [37] Han XG, Gong YH, Fu K, He XF, Hitz GT, Dai JQ, Pearse A, Liu BY, Wang H, Rublo G, Mo YF, Thangadurai V, Wachsman ED, Hu LB. Negating interfacial impedance in garnet-based solid-state Li metal batteries. *Nat Mater* 2017;16(5): 572. <https://doi.org/10.1038/nmat4821>.
- [38] Luo W, Gong YH, Zhu YZ, Li YJ, Yao YG, Zhang Y, Fu K, Pastel G, Lin CF, Mo YF, Wachsman ED, Hu LB. Reducing interfacial resistance between garnet-structured solid-state electrolyte and Li-metal anode by a germanium layer. *Adv Mater* 2017; 29(22). <https://doi.org/10.1002/adma.201606042>.
- [39] Mauger A, Armand M, Julien CM, Zaghik K. Challenges and issues facing lithium metal for solid-state rechargeable batteries. *J Power Sources* 2017;353:333–42. <https://doi.org/10.1016/j.jpowsour.2017.04.018>.
- [40] Huang S, Tang L, Najafabadi HS, Chen S, Ren Z. A highly flexible semi-tubular carbon film for stable lithium metal anodes in high-performance batteries. *Nano Energy* 2017;38:504–9. <https://doi.org/10.1016/j.nanoen.2017.06.030>.
- [41] Shen F, Zhang F, Zheng Y, Fan Z, Li Z, Sun Z, Xuan Y, Zhao B, Lin Z, Gui X, Han X, Cheng Y, Niu C. Direct growth of 3D host on Cu foil for stable lithium metal anode. *Energy Storage Mater* 2018;13:323–8. <https://doi.org/10.1016/j.ensm.2018.02.005>.
- [42] Meng Q, Deng B, Zhang H, Wang B, Zhang W, Wen Y, Ming H, Zhu X, Guan Y, Xiang Y, Li M, Cao G, Yang Y, Peng H, Zhang H, Huang Y. Heterogeneous nucleation and growth of electrodeposited lithium metal on the basal plane of single-layer graphene. *Energy Storage Mater* 2019;16:419–25. <https://doi.org/10.1016/j.ensm.2018.06.024>.
- [43] Fu KK, Gong YH, Liu BY, Zhu YZ, Xu SM, Yao YG, Luo W, Wang CW, Lacey SD, Dai JQ, Chen YN, Mo YF, Wachsman E, Hu LB. Toward garnet electrolyte-based Li metal batteries: an ultrathin, highly effective, artificial solid-state electrolyte/metallic Li interface. *Sci Adv* 2017;3(4). <https://doi.org/10.1126/sciadv.1601659>.
- [44] Luo W, Gong YH, Zhu YZ, Fu KK, Dai JQ, Lacey SD, Wang CW, Liu BY, Han XG, Mo YF, Wachsman ED, Hu LB. Transition from superlithiophobicity to superlithiophilicity of garnet solid-state electrolyte. *J Am Chem Soc* 2016;138(37): 12258–62. <https://doi.org/10.1021/jacs.6b06777>.
- [45] Huo HY, Luo J, Thangadurai V, Guo XX, Nan CW, Sun XL. Li₂CO₃: a critical issue for developing solid garnet batteries. *ACS Energy Lett* 2020;5(1):252–62. <https://doi.org/10.1021/acseenergylett.9b02401>.
- [46] Huo HY, Chen Y, Zhao N, Lin XT, Luo J, Yang XF, Liu YL, Guo XX, Sun XL. In-situ formed Li₂CO₃-free garnet/Li interface by rapid acid treatment for dendrite-free solid-state batteries. *Nano Energy* 2019;61:119–25. <https://doi.org/10.1016/j.nanoen.2019.04.058>.
- [47] Jin C, Sheng O, Luo J, Yuan H, Fang C, Zhang W, Huang H, Gan Y, Xia Y, Liang C, Zhang J, Tao X. 3D lithium metal embedded within lithiophilic porous matrix for stable lithium metal batteries. *Nano Energy* 2017;37:177–86. <https://doi.org/10.1016/j.nanoen.2017.05.015>.
- [48] Li H, Yin H, Wang K, Cheng S, Jiang K, Sadoway DR. Liquid metal electrodes for energy storage batteries. *Adv Energy Mater* 2016;6(14). <https://doi.org/10.1002/aenm.201600483>.
- [49] Armand M, Tarascon JM. Building better batteries. *Nature* 2008;451(7179):652–7. <https://doi.org/10.1038/451652a>.
- [50] Lang J, Liu K, Jin Y, Long Y, Qi L, Wu H, Cui Y. A molten battery consisting of Li metal anode, AlCl₃-LiCl cathode and solid electrolyte. *Energy Storage Mater* 2020; 24:412–6. <https://doi.org/10.1016/j.ensm.2019.07.027>.
- [51] Yang Z, Zhang J, Kintner-Meyer MCW, Lu X, Choi D, Lemmon JP, Liu J. Electrochemical energy storage for green grid. *Chem Rev* 2011;111(5):3577–613. <https://doi.org/10.1021/cr100290v>.
- [52] Xu J, Liu K, Jin Y, Sun B, Zhang ZL, Chen Y, Su DW, Wang GX, Wu H, Cui Y. A garnet-type solid-electrolyte-based molten lithium-molybdenum-iron(II) chloride battery with advanced reaction mechanism. *Adv Mater* 2020;32(32). <https://doi.org/10.1002/adma.202000960>.
- [53] Li G, Lu X, Kim JY, Viswanathan VV, Meinhardt KD, Engelhard MH, Sprenkle VL. An advanced Na-FeCl₂ ZEBRA battery for stationary energy storage application. *Adv Energy Mater* 2015;5(12). <https://doi.org/10.1002/aenm.201500357>.
- [54] Chu S, Majumdar A. Opportunities and challenges for a sustainable energy future. *Nature* 2012;488(7411):294–303. <https://doi.org/10.1038/nature11475>.
- [55] Chu S, Cui Y, Liu N. The path towards sustainable energy. *Nat Mater* 2017;16(1): 16–22. <https://doi.org/10.1038/nmat4834>.
- [56] Lu X, Lemmon JP, Kim JY, Sprenkle VL, Yang Z. High energy density Na-S/NiCl₂ hybrid battery. *J Power Sources* 2013;224:312–6. <https://doi.org/10.1016/j.jpowsour.2012.09.108>.
- [57] Li L, Xu C, Chang R, Yang C, Jia C, Wang L, Song J, Li Z, Zhang F, Fang B, Wei X, Wang H, Wu Q, Chen Z, He X, Feng X, Wu H, Ouyang M. Thermal-responsive, super-strong, ultrathin firewalls for quenching thermal runaway in high-energy battery modules. *Energy Storage Mater* 2021;40:329–36. <https://doi.org/10.1016/j.ensm.2021.05.018>.
- [58] Lin YC, Chong CH, Ma LW, Li Z, Ni WD. Quantification of waste heat potential in China: a top-down societal waste heat accounting model. *Energy* 2022;261. <https://doi.org/10.1016/j.energy.2022.125194>.